DRDC-RDDC-2017-P033

Fifth International Symposium on Marine Propulsion
SMP'17, Espoo, Finland, June 2017

A RANS-BEM coupling procedure for calculating the effective wakes of ships and submarines

David Hally

Defence Research and Development Canada, Dartmouth, NS, Canada

ABSTRACT

A RANS-BEM coupling method is described in which the action of the propeller in the RANS solution is modelled using both force and mass density fields. Comparison between the RANS and BEM solution is done at points between the propeller blades and the inflow to the BEM solution is allowed to vary in the axial direction. The difference between RANS and BEM solutions in open water is used to correct the BEM inflow. The method is illustrated using self-propulsion calculations of the BB2 submarine.

Keywords

RANS-BEM coupling; effective wake; BB2 submarine; OpenFOAM; PROCAL

1 INTRODUCTION

Although full Reynolds-averaged Navier Stokes (RANS) solutions of a propeller operating behind a ship are becoming more and more common, coupling a RANS solver for the flow around the ship with a solver using the Boundary Element Method (BEM) for the propeller is an attractive alternative since far less CPU time is required. In the coupling scheme, the influence of the propeller on the RANS solution is usually introduced via a force field mimicking the action of the propeller; the influence of the hull on the BEM solution is introduced via an inflow wake calculated from the RANS solution but from which the propeller induction calculated by the BEM solver has been subtracted. As described by Hally (2015), the changes in the flow field cause by the physical bulk of the propeller blades can also be taken into account by using a mass density field in addition to the force field in the RANS solver. Several iterations of RANS and BEM solutions are made until the BEM inflow wake (the effective wake) no longer changes significantly.

This paper will describe a RANS-BEM method implemented using the open source RANS solver OpenFOAM® version 2.1.0 and a modified version of the BEM solver PROCAL developed by the Cooperative Research Ships organization. However, many of its features could be applied with other RANS and BEM solvers.

2 POTENTIAL FLOW THEORY

In the Boundary Element Method, the velocity field, $\mathbf{v}$, is assumed to be of the form

$$\mathbf{v} = \mathbf{V} + \nabla\phi \tag{1}$$

where $\mathbf{V}$ is a known velocity field and the velocity potential, ϕ, satisfies $\nabla^2\phi = 0$. Using Green's Second Theorem, the equation for ϕ can be written as a Fredholm integral equation of the second kind:

$$-4\pi\phi = \int_S \left(\Delta\phi\frac{\partial G}{\partial n} - G\frac{\partial\Delta\phi}{\partial n}\right) da \tag{2}$$

where S is the surface of a body in the flow, G is a Green function for the Laplacian, $\partial/\partial n$ denotes a derivative in the direction of an outward pointing normal to the surface and $\Delta\phi = \phi_o - \phi_i$ is the difference between the values of the potential on the outer and inner surfaces of the body. Equation (2) is often rewritten as

$$\phi = \int_S \left(\sigma G - \mu\frac{\partial G}{\partial n}\right) da;\ \sigma = \frac{1}{4\pi}\frac{\partial\Delta\phi}{\partial n};\ \mu = \frac{\Delta\phi}{4\pi} \tag{3}$$

with σ known as the source strength and μ the dipole strength. The condition that there be no flux of fluid through the surface of the body requires that

$$\frac{\partial\phi_o}{\partial n} = -\hat{n}\cdot\mathbf{V} \tag{4}$$

on the outer surface of the body, where $\hat{n}$ is an outward pointing normal to the surface.

Equation (2) is valid for the flow inside and outside of the body. If one is only interested in the flow outside the body, it is possible to prescribe the values of either σ or μ arbitrarily; provided that the no-flux condition is satisfied, the choice will affect only the flow inside the body. In the Morino formulation (Morino et al. 1975), the source strength is chosen to be

$$\sigma = -\frac{\hat{n}\cdot\mathbf{V}}{4\pi} \tag{5}$$

On the inside surface, $\partial\phi_i/\partial n = 0$ implying that ϕ is constant, and consequently $\mathbf{v} = \mathbf{V}$, everywhere inside the body.

Figure 1 demonstrates that this is true in practice as well as in theory. It shows the induced axial velocity component computed by the BEM program PROCAL along a line of constant radius passing through the propeller of the KRISO Container Ship (KCS) operating behind the ship. At points inside the blades, the induced velocity drops to zero.

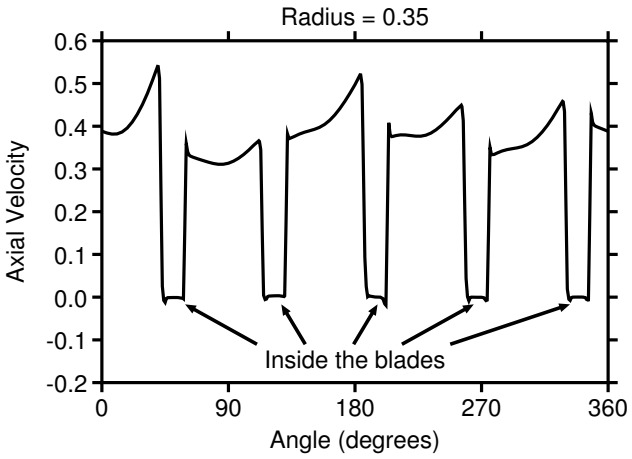

Figure 1: Normalized axial velocity for the KCS propeller at $r = 0.35R$ and $0.1R$ upstream of the propeller plane.

3 ACCOUNTING FOR BLADE BLOCKAGE USING MASS SOURCES

If, in the RANS solution, the propeller is modelled using only a force density field, then the effect on the flow of the physical bulk of the blades—the blade blockage—is ignored. Failure to account for the blade blockage when matching the RANS and BEM solutions can cause numerical errors of a few percent in K_T and K_Q; it also causes an overprediction of the thrust deduction of 5–10% leading to an error in the resistance of about 1% (Hally 2015).

One way to account for the blade blockage is to represent the blades in the RANS solution by a mass source field as well as a force density field. The mass source field is determined from the source strengths in the BEM solution which, as described above, are proportional to the mass flux through the blade surfaces caused by the inflow $\mathbf{V}$. In effect, the RANS solution now mimics the BEM flow both inside and outside of the blades. In the RANS solver, the mass source field generates source terms in both the continuity equation and the momentum equations:

$$\nabla \cdot \mathbf{v} = M; \tag{6}$$

$$\nabla \cdot (\mathbf{v}\mathbf{v}) = -\frac{\nabla p}{\rho} + \nabla \cdot (\nu_t \nabla \mathbf{v}) + M\mathbf{v} + \boldsymbol{F} \tag{7}$$

where M is the mass source field and $\boldsymbol{F}$ is the force density field. Hally (2015) describes how to implement the mass sources in OpenFOAM as well as algorithms for calculating the mass source and force density fields from the blade pressures and velocities generated by a BEM program.

4 RANS-BEM COUPLING

The basic algorithm RANS-BEM coupling algorithm is as follows.

1. Calculate the nominal wake, $\mathbf{v}_n(x, r, \theta)$, using the RANS solver. (We use cylindrical coordinates in which x increases forward along the propeller axis.)

2. Set $i = 0$ and the effective wake, $\mathbf{v}^0_{\text{eff}}(x, r, \theta)$, to the nominal wake.

   Repeat until the change in the effective wake is small enough:

   (a) Run the BEM program with $\mathbf{v}^i_{\text{eff}}(x, r, \theta)$ as inflow and use it to calculate the time averaged total wake $\mathbf{v}^i_{\text{BEM}}(x, r, \theta)$.

   (b) Calculate the propeller induction by subtracting the effective wake from the BEM total wake:

   $$\mathbf{v}^i_{\text{ind}}(x, r, \theta) = \mathbf{v}^i_{\text{BEM}}(x, r, \theta) - \mathbf{v}^i_{\text{eff}}(x, r, \theta) \tag{8}$$

   (c) Calculate the time-averaged force and mass density fields implied by the BEM.

   (d) Run the RANS solver with the force and mass density fields and use them to calculate the total wake, $\mathbf{v}^i_{\text{RANS}}(x, r, \theta)$.

   (e) Update the effective wake by subtracting the propeller induction from the RANS total wake.

   $$\mathbf{v}^{i+1}_{\text{eff}}(x, r, \theta) = \mathbf{v}^i_{\text{RANS}}(x, r, \theta) - \mathbf{v}^i_{\text{ind}}(x, r, \theta) \tag{9}$$

It is not strictly necessary to average in time but, if not done, the RANS calculations become unsteady, the CPU times necessary for the solution become much longer, and much of the attraction of the RANS-BEM method is lost.

Equations (8) and (9) can be combined to write the update of the effective wake as

$$\mathbf{v}^{i+1}_{\text{eff}}(x, r, \theta) = \mathbf{v}^i_{\text{eff}}(x, r, \theta) + \Delta\mathbf{v}(x, r, \theta) \tag{10}$$

with

$$\Delta\mathbf{v}(x, r, \theta) = \mathbf{v}^i_{\text{RANS}}(x, r, \theta) - \mathbf{v}^i_{\text{BEM}}(x, r, \theta) \tag{11}$$

To perform the update, the RANS and BEM solutions are sampled at a set of comparison points. The current approximation to the effective wake is then known at those points. Interpolation and/or extrapolation is then used to generate an inflow in the form suitable for the BEM solver.

5 COMPARISON POINTS BETWEEN THE BLADES

A common choice for the comparison points is to place them in one or more planes upstream of the leading edges of the blades. The effective wake on these planes is then extrapolated to generate the effective wake at the propeller disk which is used as the BEM inflow: see, for example, Hally (2015) or Rijpkema et al. (2013).

In the current method, the time-averaged RANS and BEM solutions are compared at points between the propeller blades. The advantage of this method is that no interpolation needs to be done to transfer the effective wake upstream to the inflow location used by the BEM solver. It also has practical advantages when there is limited space between the leading edges of the blades and the hull or

when the hub diameter is changing significantly with axial location.

Since the BEM flow field is not well-behaved near the edges of the blade panels, care must be taken to keep points where the flow field is sampled away from the panel edges. The simplest way to do this is to make the sampled points rotate with the propeller; if they are well-located on the first time step, they will also be well-located on subsequent time steps.

Suppose $\{(x, r, \theta_i) : i \in [1, N]\}$ is a series of sampled points along a circle around the axis: see Figure 2. Because the points are rotating with the propeller, as time marches forward through one rotation period, the points sweep out a lattice in (θ, t)-space similar to that shown in Figure 3 for a two-bladed propeller. Each horizontal line of points represents the line of sampled points at a single time step. The diagonal grey lines are swept out by points lying on the surface of the blades and the grey points between them are inside the blades. To perform a time average of the induced velocities at a given value of θ, say θ_0, the values are interpolated in θ at each time step (see the squares in Figure 3), then averaged over the interpolated values. The result is the averaged velocity at (x, r, θ_0).

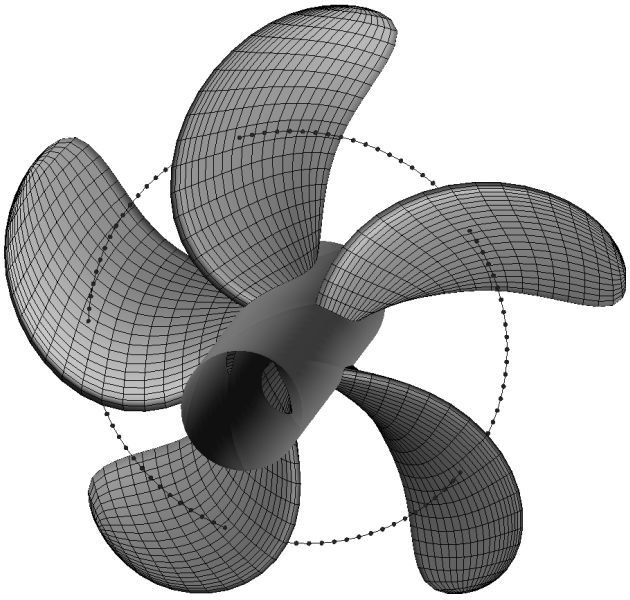

Figure 2: A line of sampled points between a pair of blades.

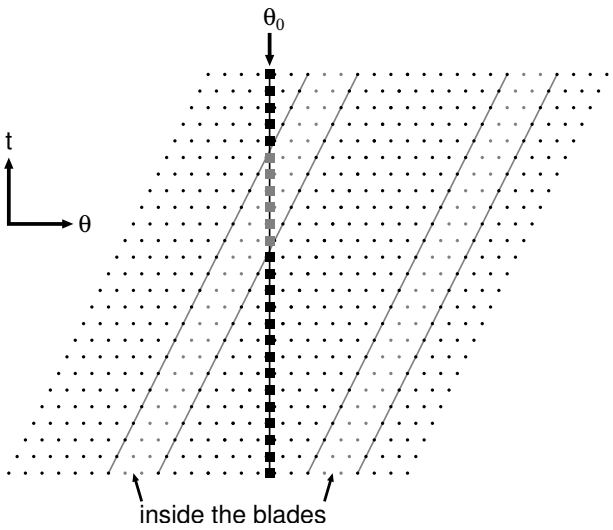

Figure 3: A single line of sampled points in (θ, t)-space.

Since the induced velocity inside the blades is zero, the points inside the blades can be thrown away and the values at any interpolation points inside the blades (the grey squares in Figure 3) set to zero.

If the points cover the full circle, it is only necessary to average in time for T/Z, where T is the period of rotation and Z is the number of blades. Alternatively, one can choose points between a single pair of neighbouring blades and average over the length of time T/Z during which θ_0 lies between the chosen blades.

In practice, the line of sampled points does not lie exactly on a circle; instead the points are placed on an arc between the centroid of a panel on the face of a blade and the centroid of the corresponding panel on the back of the next blade. This choice ensures that the points are not too close to the edges of any panel. However, it does mean that the x and r values of the points vary a little. The time-averaged velocity for the points is ascribed to the point at $(x_{\text{avg}}, r_{\text{avg}}, \theta_0)$ where x_{avg} and r_{avg} are the averages of x and r at the two panel centroids.

Each line of points as described above can be time-averaged at arbitrary values of θ; usually N_θ equally spaced values between 0 and 2π are chosen. One then knows the induced velocities at $(x_{\text{avg}}, r_{\text{avg}}, \theta_i)$. To generate a full description of the induced velocity over the propeller disk, we use many such lines of points. If the axial variation of the velocities is not considered important, then we use lines at the centroids of a single row of panels extending from the root of the blade to the tip: see Figure 4. If the axial variation of the velocities is important, several such

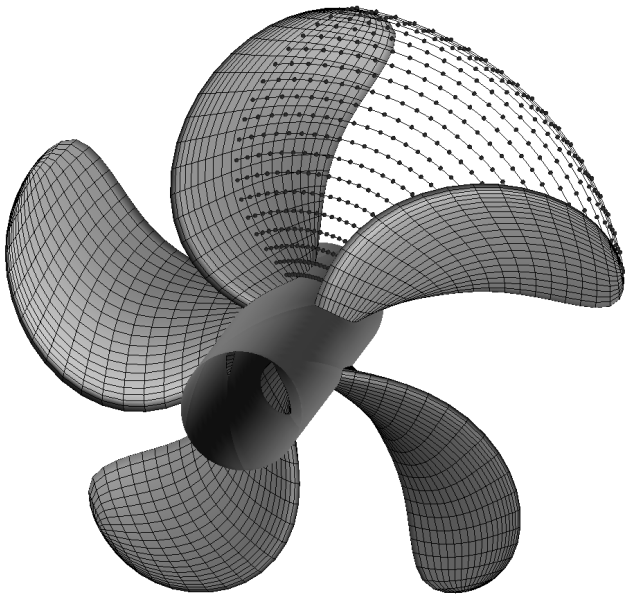

Figure 4: Sampled points generated by a single row of panels.

rows of panels are used to generate a grid of values which nearly covers the swept volume of the blades. We typically use rows of panels which are roughly 10%, 50% and 90% of the distance from the leading edge to the trailing edge. The values can be interpolated to determine the value of the induced velocity anywhere in the swept volume of the blades; some extrapolation is needed for points close to the leading and trailing edges.

Figure 5 compares the induced velocities along the blade generator line of the KCS propeller operating in open water. The PROCAL induced velocities were calculated as described above. The OpenFOAM velocities were calculated using mass and force density fields generated from the PROCAL calculation. In theory, the induced velocities should match. Note that use of the mass density field is crucial if a good match between the RANS and BEM flows is to be obtained.

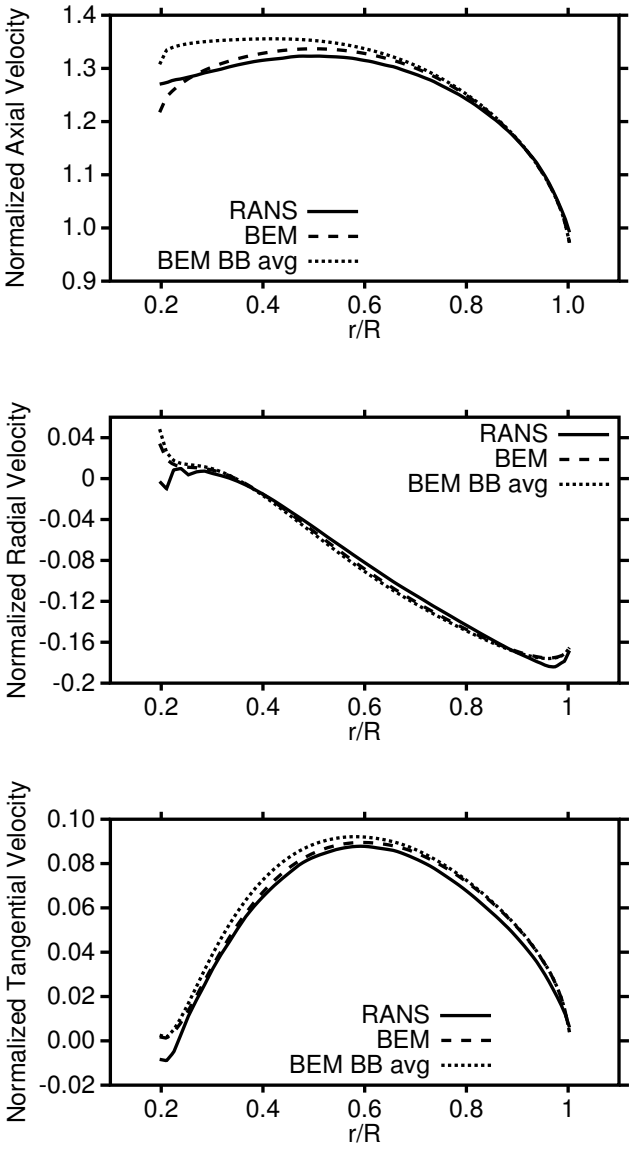

Figure 5: Comparison of the RANS and BEM velocities in the surface swept out by the generator line: KCS in open water; $J = 0.7483$.

In Figure 5, the curve labelled "BEM BB avg" was generated by averaging the velocity components only over the time that the averaging point is between the blades and not inside them. It can be seen that the axial and tangential components are then overestimated at the lower radii where the sections are thickest. The average should include the times when the point is inside the blades as shown in curve labelled "BEM".

The RANS-BEM coupling procedure was applied to the KCS propeller operating in open water with $J = 0.7438$. In theory, the effective wake should simply be the uniform inflow and the thrust and torque should not change between RANS-BEM iterations. The new method of sampling between the blades was used as well as the method described by Hally (2015) in which the wake in upstream planes are extrapolated to the propeller plane; three wakes were used at $0.3R$, $0.35R$ and $0.4R$ upstream of the propeller disk. Four iterations were performed with the value of K_T changing by less than 0.1% between the third and fourth iterations. The percent differences in K_T, K_Q and η from their open water values are tabulated in Table 1.

Table 1: The percent error in K_T, K_Q and η from each calculation method.

	K_T	K_Q	η
Old method	-2.5%	-1.7%	0.21%
New method	2.0%	1.5%	0.26%

The accuracy of the two methods is about the same with each giving a difference in K_T of about 2%. For reasons that are not understood, the OpenFOAM prediction of the propeller induction upstream of the propeller tends to be larger than the PROCAL prediction, especially at lower advance ratios. This has been found to be true for a wide variety of propellers. The larger RANS induction causes an overprediction of the effective wake and consequently an underprediction of the thrust and torque.

On the other hand, sampling the flow between the blades overpredicts K_T for reasons that are not yet clear. It is not yet known whether this will be true in general or whether it will be different for other propellers.

6 THE EFFECT OF AXIAL VARIATION OF THE WAKE

It is common in BEM propeller programs to assume that the inflow velocity, **v**, is given in a single plane and does not vary in the axial direction. This is typically the only information about the velocity field when it is determined from a wake survey. However, the procedure described in the previous section allows the possibility of representing a wake which varies over the whole of the swept volume of the blades. Since there is some extra computational effort required to generate and evaluate a wake of this type, a simple test was performed to estimate the size of the error incurred by using a wake which does not vary axially.

PROCAL was used to calculate the thrust and torque of several different propellers when the inflow was generated from the nominal wake at different locations. The nominal wake behind each vessel was calculated using the RANS

solver ANSYS® CFX®. In each case, the thrust, torque and efficiency were calculated using non-axially-varying inflows generated by sampling the nominal wake at one of three surfaces swept out by the leading edge, the generator line, or the trailing edge. The thrust, torque and efficiency were also calculated using the axially varying inflow obtained by interpolating between the nominal wake values at these surfaces. For the latter calculation, it was necessary to modify PROCAL so that it would perform the interpolation to generate the axially varying inflow.

The results from three different propellers operating in the nominal wakes of three different vessels—the KCS, the BB2 submarine and a patrol ship—are shown in Figure 6. It plots the percent difference in K_T between the results from the non-axially-varying wakes and the axially varying wake. The differences are given as a function of the location of the surfaces used for the non-axially-varying wakes. Because the hub radius near the leading edge of BB2 is significantly larger than at the trailing edge, extrapolation of the wake at the inner radii was required. This caused the calculation not to converge for the forwardmost wake.

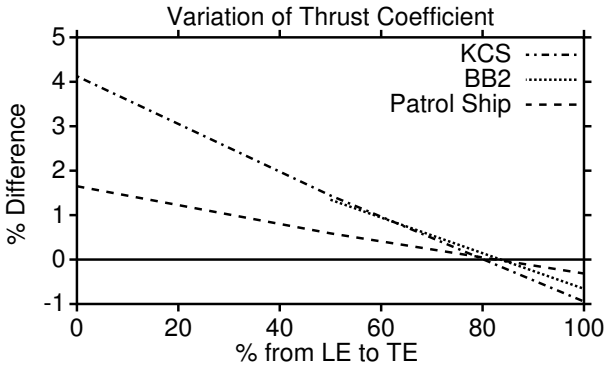

Figure 6: Percent difference in K_T between a non-axially varying wake and an axially varying wake as a function of the location of the wake plane.

When compared to calculations in which the inflow is sampled only at the generator line (or at the propeller plane, which typically gives similar results), K_T and K_Q calculated with the axially varying wake are generally reduced by 1 or 2%. When it is necessary to use an inflow at one axial location, either for reasons of efficiency or due to the limitations of the BEM solver, Figure 6 suggests that the blade generator line is the best location to use for predicting thrust is roughly 80% of the distance between the leading and trailing edges. This is in general agreement with airfoil theory which suggests that the flow over the trailing edge is most important for the determination of the lift. This also explains why K_T and K_Q is overpredicted if the comparison location is further forward; since the flow is generally accelerating through the propeller plane, the effective value of J decreases as one moves aft toward the trailing edge.

7 CORRECTING FOR THE RANS-BEM MISMATCH

In theory, for a propeller in open water, the flow fields generated by the RANS and BEM solvers should be the same so that $\Delta\mathbf{v} = 0$ and the effective wake is equal to the inflow. For these calculations it is necessary to use a slip boundary condition on the hub in the RANS solution. In practice, the two flow fields will not match exactly and their difference will introduce an error into the effective wake. The mismatch tends to increase with the loading of the propeller.

The open water mismatch can be used to provide a correction applied during the RANS-BEM coupling. To implement the correction, Equation (10) is modified to

$$\mathbf{v}_{\text{eff}}^{i} = \mathbf{v}_{\text{eff}}^{i-1} + \Delta\mathbf{v} - \delta\mathbf{v} \tag{12}$$

The correction factor, $\delta\mathbf{v}$, is determined from the difference in the RANS and BEM velocity fields in open water. The correction factor can be calculated once for one or more advance coefficients, then interpolated in J during the RANS-BEM iteration to determine an appropriate correction.

This procedure is similar to that described by Sánchez-Caja et al. (2015). They suggest that a single multiplicative correction factor, independent of J, can be used provided that the velocity components are not too small. However, in the current method, it is often the case that small velocity components arise, especially near the hub, so the procedure described above is preferable.

7.1 Accounting for the hub

In calculating the correction $\delta\mathbf{v}$, it is possible to include a non-cylindrical hub but one must use some care. First, it is necessary to ensure that the RANS solution using a slip boundary condition at the hub surface is an accurate match to the potential flow solution past the hub. A poor match will be obtained if the hub terminates abruptly so that the RANS solution separates or if other viscous effects are present.

A more subtle problem is that the uniform inflow in the open water BEM solution causes a flux of fluid through the footprint of the blades (in the interior of the propeller). However, in the RANS solution the blade footprints are closed off so that there is no flux. In consequence, the radial velocity near the blade roots will not match well between the two solutions.

Another way of looking at this problem is that the mass density field calculated from the flux through the blade surfaces will not sum to zero; it will be in error by the amount of flux through the blade footprints. When transferred to the RANS calculation, there will be a source of mass near the blade footprints which causes the radial velocity to be overestimated.

The problem can be corrected in different ways:

1. Add mass source terms to the RANS solution to account for the flux through the footprint in the BEM solution. This can be done simply by adding extra panels on the footprint of the blades and assigning them zero pressure. They will then contribute to the mass density field but not to the force field.

2. Modify the RANS boundary condition near the blade footprints to include a flux of through the footprints. This requires the ability to generate a custom boundary condition in the RANS solver.

3. Modify the inflow velocity, **v**, so that it does not cause a flux through the footprints of the blades. This is most easily done by calculating the flow over the hub alone, either using the BEM solver or the RANS solver with a slip boundary condition on the hub, then using that solution as inflow to the BEM calculation with the propeller. This method requires the BEM solver to represent the velocity field over the full extent of the blade footprint. If the radial component of the velocity changes significantly over the blade footprint, the axial variation of the wake may have to be taken into account. Since the nominal flow over the hub must be calculated, an additional RANS solution is also required.

The first method is the simplest to implement as it only requires adding a few extra panels to close the footprint of the blades.

This problem can also be present in the RANS-BEM iteration if the representation of the inflow allows some flux of fluid through the blade footprint, for example, if the wake does not vary axially but the hub does.

8 BB2

The RANS-BEM method was used to calculate the self-propulsion point of the BB2 submarine model (Overpelt et al. 2015) which was designed by DSTO in Australia and for which extensive free-swimming manœuvring tests were performed at MARIN in the Netherlands. The BB2 model is 3.826 m long and was fitted with a six-bladed MARIN stock propeller (MARIN 7371R). The hull and propeller geometries and the test data are available from the MARIN web site (BB2 data set). BB2 is shown in Figure 7.

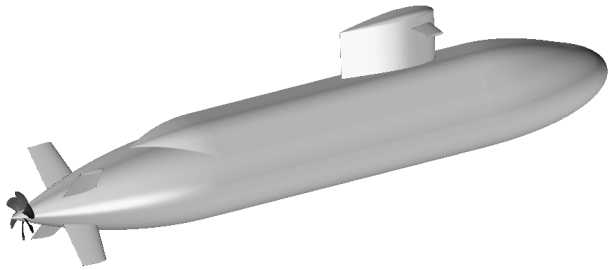

Figure 7: The BB2 submarine.

A grid for BB2 was created using the meshing software Pointwise®. It has structured blocks in the vicinity of the hull but unstructured tetrahedral blocks in the far field. The propeller is wholly contained within the structured blocks. There are 13 million nodes and 25 million cells (10 million in the structured blocks, 15 million in the unstructured blocks). The outer boundary is a cylinder extending one ship length upstream and downstream of the hull and one ship length in radius. On the hull, the mean y^+ is 0.5, on the sail and tail planes the mean y^+ is 0.8, and on the sail plane it is 1.2. The maximum value of y^+ is 3 on the hull, 4 on the sail and tail planes, and 5 on the sail plane.

For the PROCAL calculations, an axisymmetric approximation to the aft portion of the submarine body was used for the hub: see Figure 8. On the blades, there were 40 panels from leading edge to trailing edge and 30 from root to tip on both the face and the back: 2400 panels per blade.

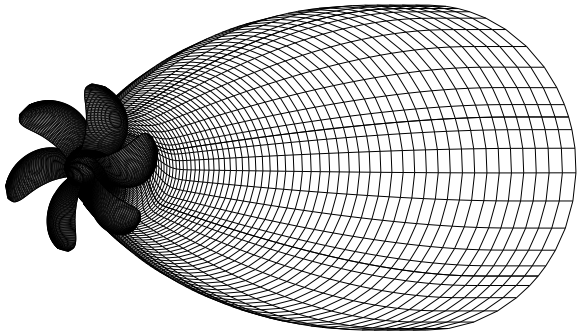

Figure 8: The panelling and hub geometry used for the BEM calculations of BB2.

The speed of the model was fixed at 1.2 m/s and, during each RANS-BEM iteration, PROCAL was required to alter the propeller rotation rate until it matched the thrust predicted by OpenFOAM.

For the RANS-BEM wake matching, the procedure described in Section 5 was used with three axial locations: at rows of panels 10%, 50% and 90% of the distance between the leading edge and trailing edge. The flow between these locations was interpolated to provide an axially varying inflow to PROCAL.

Corrections for the RANS-BEM mismatch were made by comparing RANS and BEM solutions over the axisymmetric hub. In this case OpenFOAM was run on a smaller grid (1.3 million hexahedral cells) with a slip boundary condition at the hub surface. When the propeller is not operating, the wake fraction at the generator line (50% between the leading and trailing edges) is $1 - w_{\text{nom}} = 0.857$ so the mean speed is $(1-w_{\text{nom}})V$. With the advance coefficient calculated as $J = (1 - w_{\text{nom}})V/nD$, the mismatch at each of the three sampling planes was calculated for three different values of J: 0.635, 0.699 and 0.777. Figure 9 shows the match in axial velocities normalized using the ship speed at $J = 0.699$ for comparison points 10% between the leading and trailing edges. Figure 10 plots the RANS-BEM mismatch for each advance coefficient at the same points.

To determine the correction, $\delta\mathbf{v}$, to be applied at a given RANS-BEM iteration, the current approximation of the effective wake was used to obtain a wake fraction, $1-w$, on the surface swept out by the generator line (50% between leading and trailing edges). It was used to generate an advance coefficient, $J_e = (1 - w)V/nD$ for the current rotation rate n. The values of $\delta\mathbf{v}$ at $J = 0.635$ and 0.777 were then interpolated linearly to obtain the the value of $\delta\mathbf{v}$ to be applied. Although Figure 10 indicates that the variation with J is not quite linear, this was considered a close enough approximation for the current purpose.

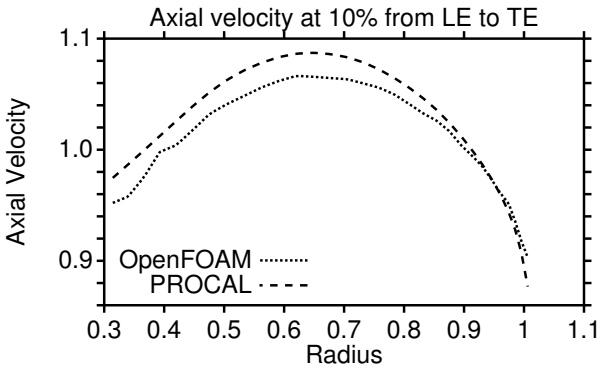

Figure 9: The axial velocities predicted by PROCAL and OpenFOAM 10% from the leading edge to the trailing edge.

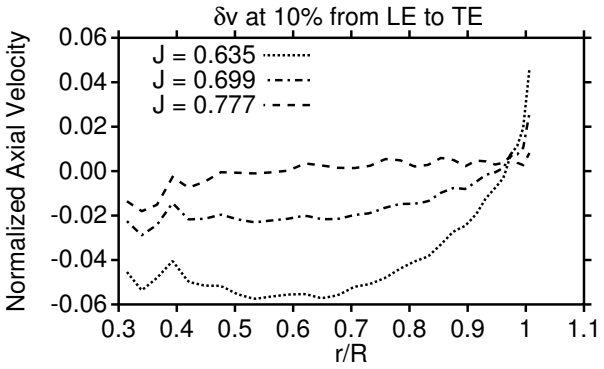

Figure 10: The RANS-BEM mismatch in axial velocity on the generator line at three advance coefficients.

Six RANS-BEM iterations were performed. For each of K_T, K_Q, rotation rate n, and effective wake fraction $1 - w_{\text{eff}}$, Figure 11 shows the percentage difference between the value at each iteration and the value on the final iteration. The nominal and effective wakes are shown in Figures 12 and 13. The irregularity in the effective wake is caused by lack of smoothness in the force and mass density fields applied to the OpenFOAM. When the RANS cells are very small, as occurs near the hull when wall functions are not used, obtaining very smooth density fields becomes very costly in CPU time but has little effect on the predictions of thrust.

The self-propulsion calculation was repeated with two variants of the RANS-BEM method:

1. with no correction for the RANS-BEM mismatch: i.e. $\delta \mathbf{v} = 0$;
2. with no correction for the RANS-BEM mismatch and with a non-axially varying wake determined at the blade generator line.

Table 2 tabulates the predictions for thrust, torque and rotation rate for the three calculations as well as the experimental values. The full RANS-BEM procedure is labelled 'Full'; the procedure with no correction for the RANS-BEM mismatch is labelled 'No corr.'; and the procedure with the axial wake is labelled 'Axial'. For ease of comparison with other predictions for this test case (Overpelt et al. 2015, Carrica et al. 2016), the values have been converted to full scale using the scaling factor $\lambda = 18.348$ and using a fluid density for sea-water of 1025 kg/m^3.

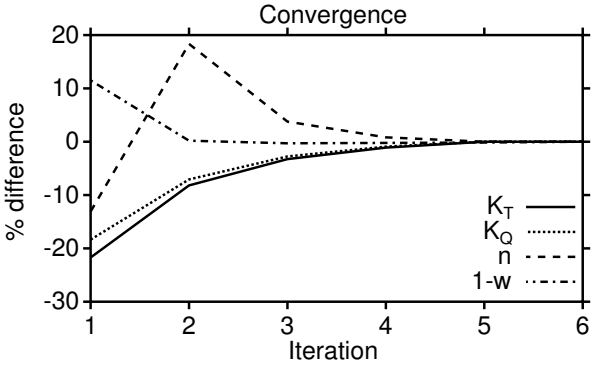

Figure 11: Convergence of the RANS-BEM iterations.

Table 2: BB2 self-propulsion characteristics for $V = 1.2$ m/s.

	Expt.	Full	No corr.	Axial
Thrust (kN)	161.5	150.5	149.4	149.8
Torque (kNm)	130.6	126.2	123.8	124.8
Rot. rate (rpm)	63.1	61.1	60.2	60.6
K_T	0.228	0.226	0.231	0.229
$10K_Q$	0.369	0.380	0.384	0.382
$1 - w_{\text{eff}}$		0.719	0.702	0.710

Like the open water calculations for the KCS discussed in Section 5, when there is no correction for the RANS-BEM mismatch, K_T is overpredicted, in this case by 1.0%. In consequence the rotation rate is lowered by 1.5%.

In the current method, the RANS-BEM iteration cannot be performed without mass sources since the update to the effective wake requires the mass sources to make the induced flow inside the blades zero. To get an estimate of the effect of the mass density field on the self-propulsion characteristics, the RANS solver was run with the mass density set to zero. The rotation rate was then calculated by PROCAL using the resistance from this calculation but without modifying the effective wake. When no mass sources were used, the resistance increased by 0.8% to 151.7 kN full scale. The rotation rate of the propeller increased by 0.2% to 61.2 rpm full scale.

9 DISCUSSION

When compared with a typical implementation of RANS-BEM coupling, the current method offers one undeniable advantage: comparing the solution between the blades avoids problems when there is little space between the hull and the propeller or when the hub shape changes rapidly making extrapolation from upstream locations difficult. The remaining implementation details all cause small corrections of the order of 1 to 2% in calculated thrust. One of the goals of this work has been to understand the effects of these corrections so that one can ensure that several 1 to 2% errors don't add up to a 5 to 10% error.

In the method described here, the blade blockage is always taken into account. In this case, failure to account

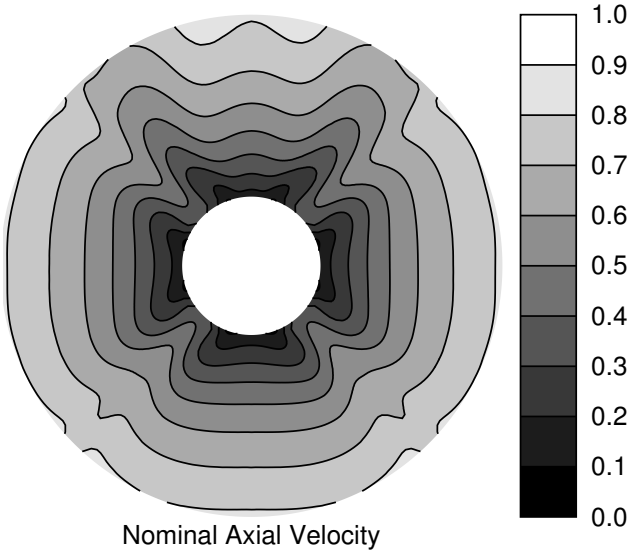

Figure 12: The BB2 nominal wake calculated by OpenFOAM.

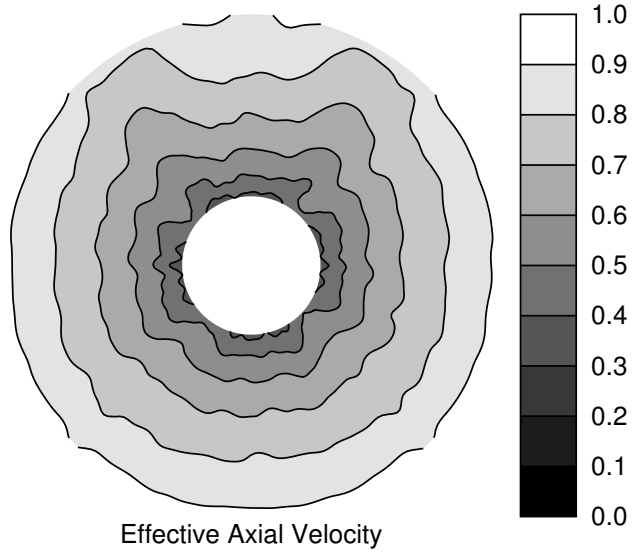

Figure 13: The BB2 effective wake calculated by OpenFOAM.

for the RANS-BEM mismatch causes an overprediction of the thrust by about 0.7% and underprediction of the rotation rate by about 1.5%. The error is within the overall accuracy of the method and less than the additional uncertainties inherent in the thrust prediction by PROCAL and the resistance prediction by OpenFOAM. However, if the propeller is operating at an off-design condition, the importance of the RANS-BEM mismatch will be greater.

The effect of the axially varying wake was not as large as was expected from the simple tests described in Section 6. This is because the acceleration of the flow through the propeller disk causes the effective wake to vary less in the axial direction than the nominal wake. Although it remains to be confirmed with more propellers, the effect of the axially variation of the wake will likely always be well within the overall accuracy of the method.

As discussed by Hally (2015), the blade blockage slows the fluid upstream of the propeller reducing the resistance of the hull, typically by about 1%. Ignoring the blade blockage means more thrust will be required and the rotation rate at the self-propulsion point will increase. Extrapolation of upstream comparison points to the propeller plane (or further) tends to underpredict the thrust also causing the rotation rate at the self-propulsion point to increase, but this effect can be compensated by correcting for the RANS-BEM mismatch in the upstream planes. Failure to correct for either effect will likely cause errors in the prediction of thrust of about 2–3%. However, if corrected, extrapolation, when possible, should perform as well as the methods described here.

ACKNOWLEDGEMENTS

The author would like to thank Johan Bosschers of MARIN for pointing out the feasibility of placing the comparison points between the blades.

REFERENCES

(2017), BB2 data set (online), MARIN, `http://www.marin.nl/web/Ships-Structures/Navy/Submarines.htm` (Access Date: Feb. 2017).

Carrica, P. M., Kerkvliet, M., Quadvlieg, F., Pontarelli, M., and Martin, J. E. (2016), CFD Simulations and Experiments of a Maneuvring Generic Submarine and Prognosis for Simulation of Near Surface Operation, In 31th Symposium on Naval Hydrodynamics, Monterey, CA, USA.

Hally, D. (2015), Propeller analysis using RANS/BEM coupling accounting for blade blockage, In Proc. of the 4th Int. Symposium on Marine Propulsors, pp. 296–303, Austin, Texas, U.S.A.

Morino, L., Chen, L.-T., and Suciu, E. O. (1975), Steady and oscillatory subsonic and supersonic aerodynamics around complex configurations, AIAA Journal, 13(3).

Overpelt, B., Nienhuis, B., and Anderson, B. (2015), Free Running Manoeuvring Model Tests on a Modern Generic SSK Class Submarine (BB2), In Pacific Int. Maritime Conference, Sydney, Australia.

Rijpkema, D., Starke, B., and Bosschers, J. (2013), Numerical simulation of propeller-hull interaction and determination of the effective wake field using a hybrid RANS-BEM approach, In Proc. of the Third Int. Symp. on Marine Propulsors, Launceston, Tasmania, Australia.

Sánchez-Caja, A., Martio, J., Saisto, I., and Siikonen, T. (2015), On the enhancement of coupling potential flow models to RANS solvers for the prediction of propeller effective wakes, J. of Marine Science and Technology, 20, 104–117.